A Stochastic Evaluation of Geothermal Reservoir Potential for the Tuscarora Sandstone in Morgantown, West Virginia, USA

Jared D. Smith[1]

[1]**Cornell University, School of Civil and Environmental Engineering, Ithaca, NY**

Keywords

Uncertainty Analysis, Sensitivity Analysis, Reservoir Productivity Index, Sedimentary Reservoir, Geothermal Direct-Use, Low-Temperature

ABSTRACT

The Tuscarora Sandstone is a target for use as a geothermal reservoir for direct-use heating of the West Virginia University campus in Morgantown. Currently, the nearest wells drilled to the Tuscarora are located about 15 km from Morgantown, and the nearest well with permeability data is about 60 km from Morgantown. As a result, there are relatively large uncertainties in geologic properties and flow geometries for the Tuscarora below Morgantown, which is common in the exploration phase of geothermal projects. This paper presents a stochastic estimation of the geothermal reservoir productivity for the Tuscarora Sandstone that accounts for these uncertainties. Statistical analyses of available geologic datasets are used to characterize probability distributions for reservoir properties, including porosity, permeability, reservoir thickness and depth. A Monte Carlo analysis of these reservoir properties and fluid properties is used to estimate the Tuscarora reservoir flow productivity. Results are compared for fracture-dominated and matrix flow productivity to estimate bounds of the favorability. A sensitivity analysis of flow productivity results explores the impact of uncertainties in engineering-controlled variables and variables whose probability distributions are not well-characterized by the available data. Transforming the reservoir productivity predictions into favorability values allows for probabilistic interpretations of the Tuscarora achieving certain favorability thresholds. The methods presented in this paper may be applied before site-specific data are collected to inform project decision making and data collection.

1. Introduction

As part of an ongoing U.S. Department of Energy-funded study, the West Virginia University campus in Morgantown is being evaluated for the feasibility to utilize deep geothermal resources for direct-use heating of campus facilities (Garapati et al., 2019; McCleery et al., 2018). The target formation for a geothermal reservoir is the Tuscarora Sandstone, which regionally has fracture-dominated permeability in hydrocarbon reservoirs (Avary, 1996). There are relatively large uncertainties in geologic properties and in the flow geometry of the Tuscarora below Morgantown. The uncertainties arise from 1) a lack of wells drilled to the depth of the Tuscarora within ~15 km of Morgantown, 2) from the long distance to the nearest well with permeability measurements (~60 km), and 3) from the limitation of permeability data to laboratory measurements on core, rather than borehole flow tests. Such uncertainties are common in the early phases of geothermal projects, and they are important to consider for probabilistic evaluations that inform project decisions (e.g. Witter et al., 2019).

This paper presents a stochastic evaluation of geothermal reservoir favorability for the Tuscarora Sandstone below Morgantown using simple metrics that estimate unstimulated reservoir productivity. Reservoir productivity is generally defined as how well a reservoir produces fluid, which is water in this paper. The stochastic method involves estimating reservoir productivity using a Monte Carlo uncertainty analysis that considers local well log data (< 30 km from Morgantown) and regional core permeability data (~60 km from Morgantown). Reservoir productivity values are computed for metrics that describe both fracture-dominated and matrix flow as bounding scenarios for the Tuscarora below Morgantown. A sensitivity analysis is presented for engineering-controlled variables (e.g. well separation distance) and for variables whose probability distributions are not well-characterized by available data. The reservoir productivity results for Morgantown are presented in the context of the Appalachian Basin reservoir favorability analysis by Camp et al. (2018), which was completed as part of the U.S. DOE-funded Geothermal Play Fairway Analysis of the Appalachian Basin (Jordan et al., 2016). Transforming the reservoir productivity results into favorability allows for probabilistic interpretations of the Tuscarora achieving specific Camp et al. (2018) favorability thresholds (e.g. unfavorable, okay, favorable).

2. Methods to Assess Geothermal Reservoir Productivity

The methods described in Camp et al. (2018) are used to estimate geothermal reservoir productivity. Those methods and reservoir productivity metrics are summarized in this section, along with additional assumptions and modifications made for this analysis. Reservoir stimulation methods that aim to improve permeability (e.g. Lu, 2018) are not considered in this paper, to be consistent with the Camp et al. (2018) analysis.

2.1 Reservoir Productivity Metrics

The permeability of the Tuscarora Sandstone is expected to be fracture dominated (Avary, 1996). Of the reservoir productivity metrics in Camp et al. (2018), the reservoir flow capacity (RFC) is most appropriate for fracture-dominated permeability. The RFC is analogous to transmissivity, and considers the (average) permeability over the thickness of the reservoir. The reservoir may have several permeable zones over its thickness, and the RFC is indifferent to the cause of the permeability (e.g. matrix, fracture). Therefore, this metric does not distinguish between different fracture flow geometries, which for the same RFC value could reflect geometries ranging from 1) a single high permeability zone that provides an undesirable short time to thermal breakthrough to 2) distributed fractures of relatively lower permeability that provide desirable heat sweep of the reservoir.

It is also possible that the Tuscarora below Morgantown provides essentially matrix flow. If matrix permeability were too low for economic extraction of thermal energy, fracture flow may be preferred. However, if matrix permeability were sufficient to meet heat transfer needs, then it may allow for greater heat sweep of a reservoir compared to fracture flow. The reservoir productivity index for water (RPI_w) is the metric used for matrix flow, which assumes a homogeneous and isotropic porous medium with a single fluid (i.e. water) produced from two vertical wells (e.g. Craft and Hawkins, 1959; Dietz, 1965; Gringarten, 1978).

Equation 1 and Equation 2 provide the RFC and the RPI_w metrics, respectively

$$\mathrm{RFC} = \mathrm{k_w H} \;\; [\,\mathrm{mD\ m}\,] \tag{1}$$

$$\mathrm{RPI_w} = \frac{2\pi\, \mathrm{k_w H}}{\mu \ln\left(\frac{\mathrm{d}}{\mathrm{r_{well}}}\right)} \rho_w \;\left[\frac{\mathrm{kg}}{\mathrm{Pa \cdot s}}\right] \tag{2}$$

where k_w is the water permeability (mD for RFC, m^2 for RPI_w), H is the thickness of the reservoir (m), μ is the dynamic viscosity of water at the temperature of the reservoir (Pa - s), ρ_w is the density of water at the temperature and pressure of the reservoir (kg/m^3), d is the distance between wells (m), and r_{well} is the inner radius of the well (m). A constant water density of 988 kg/m^3 is used to be consistent with the reservoir analysis presented in Camp et al. (2018). Further details about these metrics are provided in Camp et al. (2018).

2.2 Klinkenberg Permeability Correction

The RFC and RPI_w metrics require the rock permeability for water. Permeability was measured using air in the dataset used in this paper (McDowell et al., 2018; Section 3.4, this paper), so a Klinkenberg correction is needed to convert the air permeability to an effective water permeability. The Klinkenberg correction used in this study is provided in Jones (1987) (regression developed for sandstones with permeability range 0.01 mD to 2000 mD). All air permeability measurements in this paper are greater than 0.01 mD. Some air permeability measurements are greater than 2000 mD, but applying the correction to such high permeabilities negligibly reduces their values.

Equation 3 provides the general form of the Jones (1987) Klinkenberg correction for effective water permeability (k_w), and Equation 4 provides the parameter specification for b

$$\mathrm{k_w} = \frac{\mathrm{k_g}}{1 + \frac{\mathrm{b}}{\mathrm{p}}} \;[\mathrm{mD}] \tag{3}$$

$$\mathrm{b} = 15.61 \left(\frac{\mathrm{k_g}}{\phi}\right)^{-0.447} [\mathrm{psig}], \qquad 0.01\ \mathrm{mD} < \mathrm{k_g} < 2000\ mD \tag{4}$$

where k_g is the gas (air) permeability (mD), ϕ is the rock decimal porosity, b is the “fractional increase in apparent permeability which would be observed when measuring k_g [with air] at atmospheric pressure” (Jones and Owens, 1980) (psig), and p is the mean flowing gauge pressure of the equipment used to measure k_g (psig). In this study, p = 26 psig using a Core Labs PPP-250 minipermeameter (McCleery et al., 2018).

The Tuscarora rock porosity is estimated from core samples in this study, as presented in Section 3.3. The average porosity is assigned to all values of permeability because sufficient porosity and permeability measurements in the same core sample locations are not available to develop a porosity-permeability regression relationship (e.g. Ehrenberg and Nadeau, 2005). For the smallest k_g measured in this dataset, 0.4 mD, using porosity values of 0.5% or 15% instead of the average value of 3% affects the correction to k_w by less than a factor of 1.2. The factor is smaller for larger values of permeability. Assuming average porosity for all k_g will not greatly impact the resulting k_w values.

2.3 Well Specifications for the RPI$_w$ Metric

The RPI$_w$ requires a well separation distance and a wellbore radius. Based on thermal-hydraulic modeling (Garapati et al., 2019), the optimal distance between injection and production wells is expected to be between 400 m and 1000 m for various scenarios evaluated for the West Virginia University campus (N. Garapati, personal communication). For consistency with Camp et al. (2018), a distance of 1000 m is assumed. The sensitivity of the RPI$_w$ results to well separation distance is evaluated using separations from 400 m to 1000 m in increments of 200 m.

The assumed inner radius of the wellbore at production depth is 0.1 m (3.93”), which is the same value used in Camp et al. (2018). The corresponding inner diameter is between the 6.2” and 8.5” values assigned to “small diameter” and “large diameter” geothermal wells in a GeoVision study by Lowry et al. (2017).

2.4 Uncertainty Analysis for RFC and RPI$_w$

To provide estimates of uncertainty in the RPI$_w$ and RFC productivity metrics, Monte Carlo analyses of the reservoir properties and fluid properties within Equation 1 and Equation 2 are implemented, as described within Camp et al. (2018). That study provides tables of uncertainty levels for variables in Equations 1 and 2. The variables considered are the reservoir thickness, reservoir permeability, and fluid viscosity. Selection of values for the mean, uncertainty level, and probability distribution for each of these properties are described in Section 3. Some probability distributions are not well-characterized from the available data, so sensitivity analysis is applied to the parameters of those distributions to evaluate the impact on the resulting reservoir favorability.

3. Estimation of Tuscarora Reservoir Properties

The following subsections present a detailed discussion of a data-driven selection of values and probability distributions for Tuscarora reservoir properties that were used in the Monte Carlo computations of reservoir productivity metrics. Reservoir properties include 1) spatial area, 2) depth and thickness, 3) porosity, 4) permeability, and 5) viscosity at depth based on estimated temperatures at depth. Permeability is estimated for fracture-dominated and matrix flow geometries. A summary of the values and probability distributions selected for the Monte Carlo analysis is provided in Table 2 in Section 4.

3.1 Estimated Areal Extent of the Tuscarora for Production near Morgantown, WV

The areal extent of the Tuscarora was estimated based on reasonable pumping distances from the production well to users in Morgantown. A 5 km pumping distance was assumed as a maximum distance in the Jordan et al. (2016) geothermal direct-use utilization analysis, and was also adopted in this paper. The Tuscarora permeability is thought to be structurally controlled (Avary, 1996), so structural features may also limit the extent of the Tuscarora within which the geologic properties are similar. A fault southeast of Morgantown that is visible on the surface is of concern because those rocks could be more fractured than the rocks near Morgantown. The extent of the Tuscarora for Morgantown was clipped to be north and west of this fault, as shown in Figure 1. Further extension or reduction of the Tuscarora areal extent may be made after more detailed local analyses are completed.

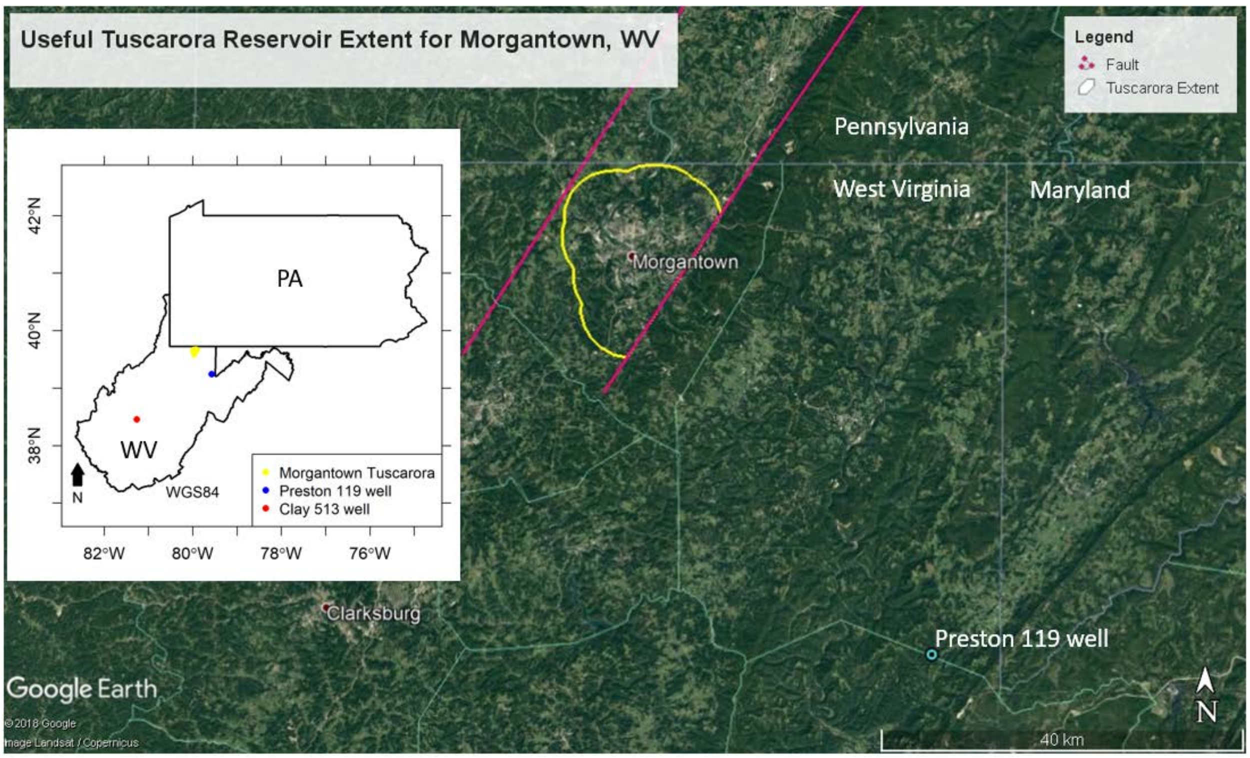

Figure 1: Estimated areal extent (yellow) of the Tuscarora Sandstone as a geothermal reservoir near Morgantown, WV. The yellow outline provides a 5 km buffer around Morgantown, as defined in the 2010 Census Incorporated Places (West Virginia GIS Technical Centers, 2010). The buffer is limited on the eastern side because of a fault (magenta).

3.2 Tuscarora Depth and Thickness

Regional geological information leads to the expectation that there is little variation in the depth and thickness of the Tuscarora within the areal extent provided in Figure 1. Based on an analysis of 5 wells within 15 km of Morgantown by McCleery et al. (2018), the thickness of the Tuscarora near Morgantown is expected to be on average 400 ft (122 m), with a true vertical depth of about 10,030 ft (3058 m) below ground surface. It is unclear if this entire thickness would be productive as a geothermal reservoir. Permeability measurements provided in Section

3.4 indicate a possibility that the deepest third of the reservoir has lower permeability than the shallower two thirds. As a result, in this paper sensitivity of the reservoir productivity results to the mean reservoir thickness is presented using a 122 m average thickness and an 83 m average thickness.

The uncertainty level (Camp et al., 2018) assigned to the Tuscarora thickness in this paper is 1, which states that ±20% of the mean thickness defines the lower and upper bounds of a symmetric triangular distribution. For a 122 m mean reservoir thickness, the bounds are [97 m, 147 m], and for the 83 m mean thickness the bounds are [66 m, 100 m]. The Tuscarora thicknesses observed in three local wells with complete Tuscarora thicknesses information are within one or both of these intervals. The Tuscarora permeability in these locations is unknown.

In Camp et al. (2018), the reservoir depth was fixed at the average oil or gas production depth. For consistency with that analysis, the depth of the Morgantown Tuscarora was assigned a fixed value of 3 km. Even a relatively large uncertainty of ±100 m depth would result in only ~±3% change in reservoir productivity.

3.3 Tuscarora Porosity for the Klinkenberg Correction

McDowell (2018) collected visual porosity estimates using blue stain on 29 rock thin sections spanning 19 m (62.3 ft) of the Tuscarora Sandstone from core from the Clay 513 well (API: 4701500513; Figure 1) in Clay County, WV (Table 1). This well is in a similar structural setting as Morgantown (McCleery et al., 2018). Porosity was estimated by comparison of thin section view(s) at the lowest available magnification (1x objective – 10x eyepiece), based on charts in Terry and Chilingar (1955) (R. McDowell, personal communication). A variety of features induce localized porosity contrasts, including stylolites, burrows, and fractures. This small sample of Tuscarora porosity is likely insufficient to fully characterize the distribution of porosity for Tuscarora reservoirs; however, this dataset (Table 1) is the largest available with which to estimate an average porosity.

Table 1: Number of McDowell (2018) samples within visual porosity classes (Terry and Chilingar, 1955) for the Tuscarora sandstone in the Clay 513 well. Four samples had zonal porosity features (e.g. matrix vs. stylolite) and have one count per feature.

Number of Samples	Visual Porosity (%)
17	≤1
5	1 to 2
4	2 to 5
5	5 to 10
1	10 to 15
1	15 to 25

Based on Table 1, the most likely value of porosity for the Tuscarora for this well is ≤ 1%. Zones of porosity > 10% result from burrows and from coarse or very coarse local grain size distributions. Fractures seem to have less impact on porosity than do burrows and grain size for this well. The minimum and maximum visual porosity estimates for core sample depths are provided in Figure 2. The porosity varies by as much as 10% within a 5 ft (~1.5 m) interval. The average low porosity is about 1.3%, the average high porosity is about 4.7%, and the overall average is about 3%. 3% porosity is assumed in the Klinkenberg permeability correction.

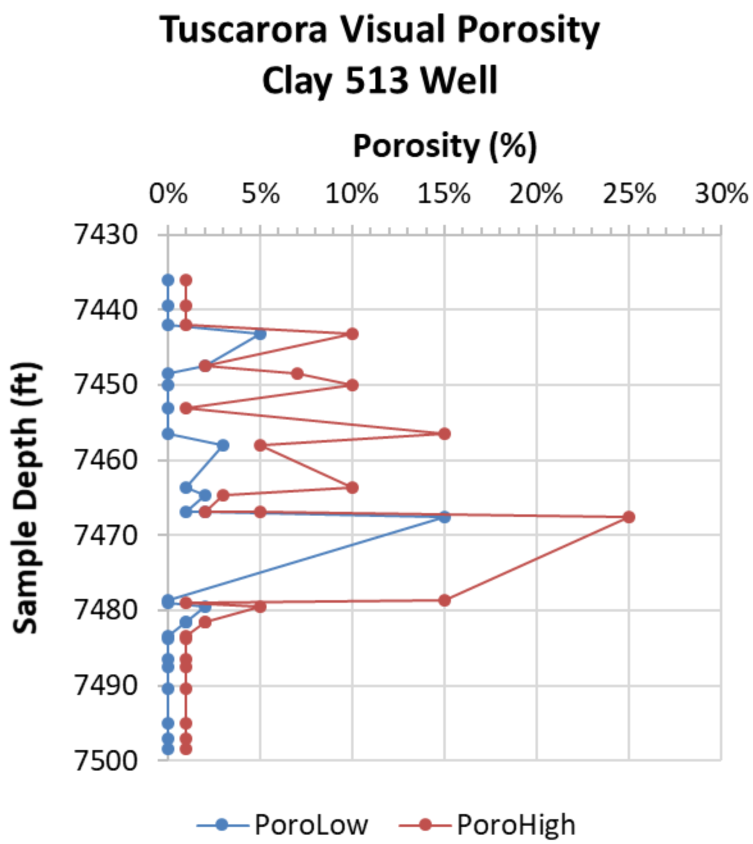

Figure 2: Low (blue) and high (red) visual porosity estimates for rock thin sections from core from the Clay 513 well (McDowell, 2018). Lines connecting sample points are for visual reference, and should not be used to infer geologic trends with depth.

3.4 Tuscarora Permeability

McDowell, Lewis, and Daft (2018) collected air permeability measurements in 753 unique locations on 279 different core samples spanning a 273 ft (83 m) thickness of the Tuscarora in the Preston 119 well (API: 4707700119; Figure 1) in Preston County, WV. Three measurements were taken in each location to estimate measurement errors resulting from the data collection method. Generally, measurement errors increase in magnitude for higher permeabilities, and errors do not seem to be significant relative to variability in permeability along the length of the core. For this analysis, the average of the three measurements is used, after converting to effective water permeability using Equations 3 and 4. Measurements taken on fractures listed as horizontal or subhorizontal with dip angles less than 20° were excluded from this analysis because these fractures are likely to be closed at the *in situ* depths of the Tuscarora.

Figure 3 provides the effective water permeability as a function of depth for this well. Permeable zones greater than 1 Darcy are found throughout the Tuscarora thickness. Filled fractures tend to have smaller permeability than unfilled fractures. Shallower depths within this well seem to have more frequent permeable zones than deeper depths.

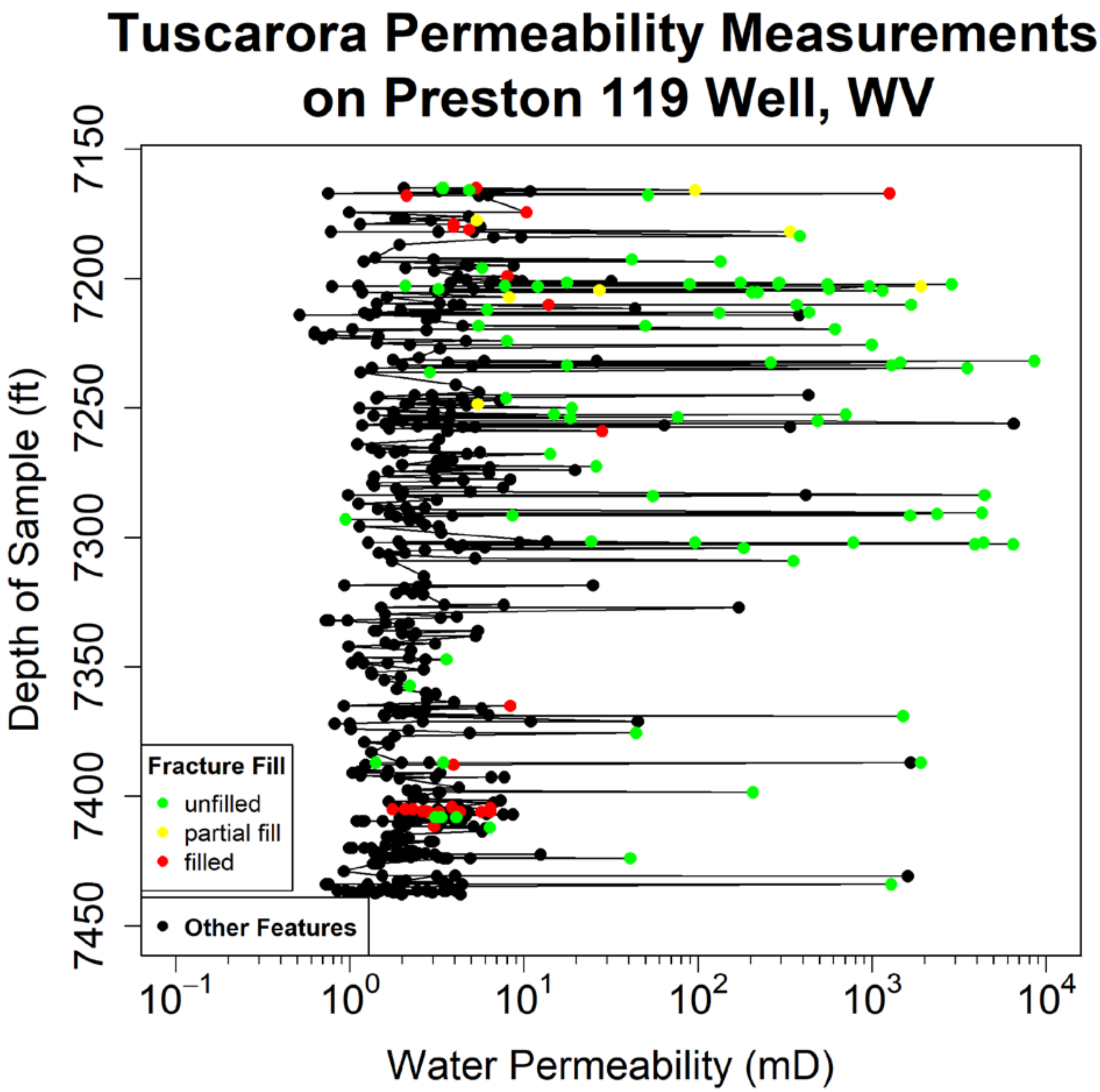

Figure 3: Tuscarora effective water permeability (mD) based on core samples from the Preston 119 well in Preston County, WV. Measurements on horizontal and subhorizontal fractures with dip angles less than 20° are not plotted. Lines connecting points are for visual aid and should not be used to infer geologic trends in permeability with depth.

Permeability measurements were taken on several structural features that are known to affect permeability. The role of the type of features can be expressed with an effective water permeability histogram (Garapati et al., 2019; Figure 4). Permeabilities less than 10 mD are found primarily in matrix rock. The following features were grouped into a Matrix Rock category to calculate the permeability in the RPI_w metric: matrix, matrix with stylolites, coarse grain with and without stylolites or voids, granular, and burrow. Matrix Rock permeability was measured on every core sample, so the resulting permeability distribution should be representative of the population Tuscarora Matrix Rock permeability over this depth range. For fracture permeability, the distribution in Figure 4 should be considered as an upper bound estimate for Morgantown because the Preston 119 well is located about 0.7 miles from the crest of the Eglon Anticline (Hennen et al., 1914), whereas Morgantown is not in a similar structural position. Based on observations from the core (R. McDowell, personal communication), this limb of the anticline seems highly fractured.

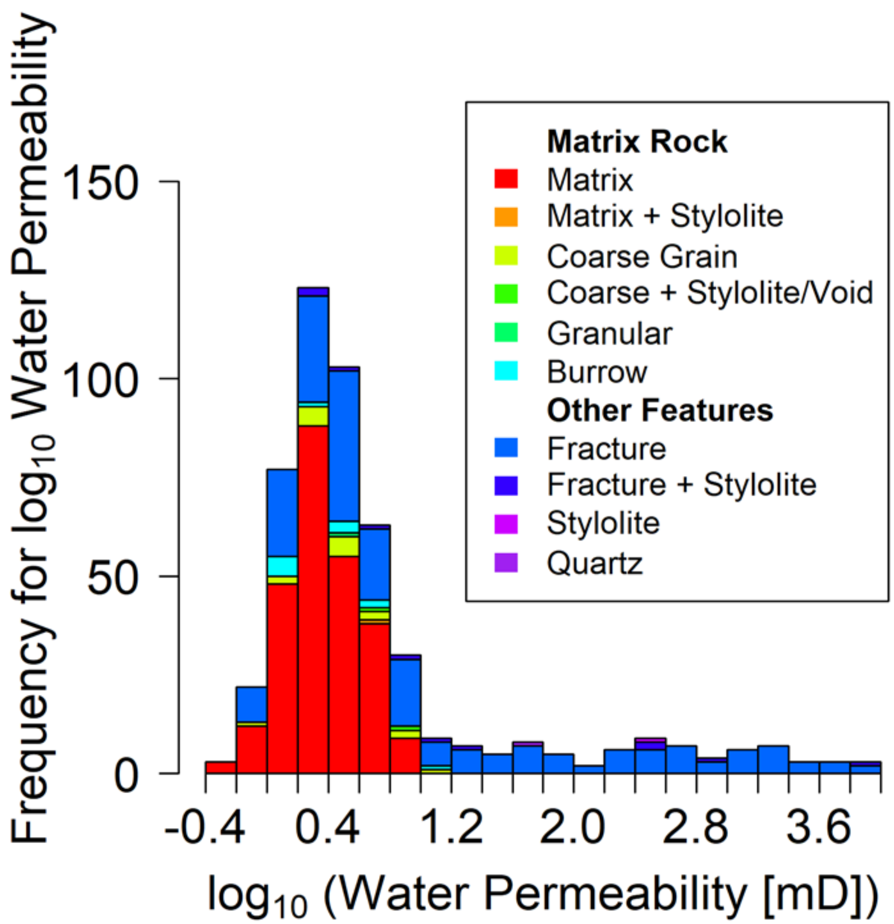

Figure 4: Stacked barplot showing the contribution to the water permeability by the type of structural feature. The aggregate distribution is the effective water permeability histogram for the samples collected. Measurements on horizontal and subhorizontal fractures with dip angles less than 20° are not plotted.

3.4.1 Matrix-dominated permeability

The observed Matrix Rock permeabilities have a real-space mean of 2.79 mD and real space standard deviation of 1.76 mD (coefficient of variation [CV] = 63%). The histogram of observed Matrix Rock water permeability (Figure 5) does not resemble an analytic distribution. The lognormal distribution is commonly used to model permeability, and it was also used in Camp et al. (2018), so it is selected for this analysis. Based on the Matrix Rock permeability data, the uncertainty level was assigned as 3, which corresponds to a lognormal distribution coefficient of variation (CV) of 50%. The resulting lognormal distribution fit to the data is displayed in Figure 5. Using the next largest uncertainty level of 4 (CV = 100%) results in the tails of the distribution being thicker in density than were observed.

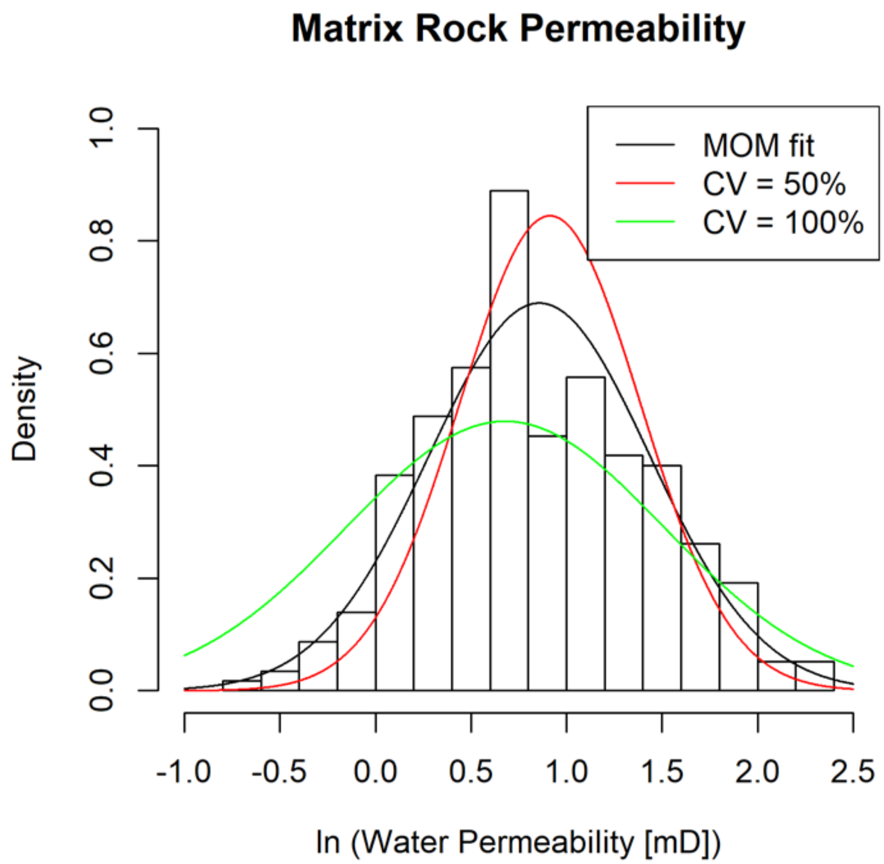

Figure 5: Lognormal distribution fit to Matrix Rock effective water permeability using the method of moments (MOM) (black) and fit assuming an uncertainty level of 3 or 4, corresponding to a CV of 50% (red) or 100% (green).

3.4.2 Fracture-dominated permeability

For the Reservoir Flow Capacity (RFC) metric, the entire distribution shown in Figure 4 was used to estimate parameters for an analytic probability distribution to describe permeability. Every structural feature on these cores was sampled (R. McDowell, 2018, personal communication), so it is assumed that the dataset is representative of the population distribution that describes Tuscarora permeability.

The RFC metric assumes a mean water permeability for the reservoir. The RFC is a simplified transmissivity calculation, so the appropriate mean permeability to use depends on the reservoir flow geometry. Because the flow geometry is unknown for the Preston-119 Tuscarora and for the Morgantown Tuscarora, this analysis evaluates each of three mean permeabilities: the arithmetic mean, geometric mean, and harmonic mean. These means provide estimates of a representative homogeneous reservoir permeability for a reservoir that is expected to be heterogeneous with the flow geometries described below. These values are not expected to perfectly represent the actual flow geometry in the Morgantown Tuscarora, although they provide bounds on the actual productivity.

The arithmetic mean considers that most of the flow will be from high permeability zones, even though they have relatively low probability density (Figure 4). The representative flow geometry is laterally extensive parallel fractures (e.g. Warren and Price, 1961). The geometric mean has been shown to reproduce the large-scale effective permeability of some reservoirs (e.g. Jensen, 1991). The harmonic mean is representative of fractures connected in series. For this study, the harmonic mean fracture-dominated permeability is similar to the average Matrix Rock permeability (Figure 5). Results are provided for Matrix Rock RFC, so the harmonic mean is not analyzed. Results are compared for the RFC for the geometric mean and arithmetic mean fracture-dominated permeabilities.

Assuming that the Preston-119 Tuscarora is representative of the Morgantown Tuscarora, a bootstrapping approach is appropriate to estimate the distribution of the mean effective water permeability. The 1D vertical autocorrelation of the effective water permeability was estimated using a variogram to inform whether or not block bootstrapping methods would be necessary to capture vertical autocorrelation in permeability (e.g. Solow, 1985). Average vertical autocorrelation did not change significantly for sample separation distances ranging from 5 ft to 100 ft (1.5 m – 30.5 m), so block bootstrapping was not used.

For the bootstrapping experiment, 100,000 random samples of size 505 were used, selected with replacement from the original sample of 505 measurements. The mean (geometric and arithmetic) of each 505-element sample was computed as an estimate of the mean effective water permeability for Tuscarora reservoirs. The resulting distribution of the mean effective water permeability is provided as a histogram in Figure 6. The bootstrapped real-space arithmetic mean of the effective water permeability is 157 mD, with a standard deviation of 33 mD (CV = 21%). The bootstrapped real-space geometric mean of the effective water permeability is 5.2 mD, with a standard deviation of 0.44 mD (CV = 9%).

A lognormal distribution fit to the bootstrapped permeability data using the Method of Moments (MOM) is provided in Figure 6, along with lognormal distributions corresponding to uncertainty levels of 1 and 2 for CVs of 12.5% and 25%, respectively. Neither of the uncertainty levels provide great fits to these bootstrapped distributions. To provide a wider range of possible values for the mean reservoir permeability, the CV of 25% is selected for the arithmetic mean, and a CV of 12.5% is selected for the geometric mean. The sensitivity of RFC results to the choice of CV is evaluated in Section 4.4.

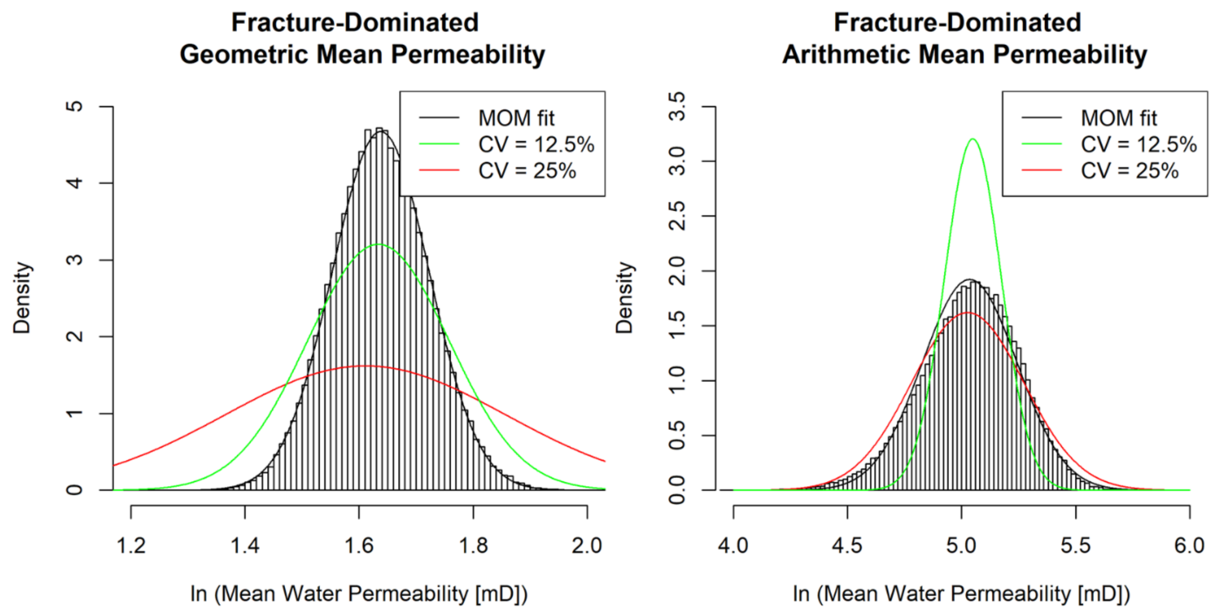

Figure 6: Lognormal distributions fit to histograms of bootstrapped random samples of the arithmetic (left) and geometric (right) mean effective water permeability. Distributions are provided using the method of moments (MOM) (black), and uncertainty levels of 1 (CV = 12.5%) (green) and 2 (CV = 25%) (red).

3.5 Fluid Viscosity at the Tuscarora Depth

For this analysis, pure water is assumed to be consistent with analyses presented in Camp et al. (2018). At the temperatures estimated at the depth of the Tuscarora below Morgantown, the viscosity of water is primarily a function of temperature.

Temperatures at depth were estimated by Smith (2019, Ch.3) as follows: 1) the surface heat flow mean and uncertainty maps from Jordan et al. (2016) were used to gather values for Morgantown, 2) a Monte Carlo analysis of geologic properties (thermal conductivity, heat generation, formation thicknesses and depths) and surface heat flow was used in a 1-D heat conduction model (Smith and Horowitz, 2017) to estimate temperatures at depth. Figure 7 provides violin plots (kernel density plots, also known as smoothed histograms, with boxplots in the center) of the temperatures at depth in 0.5 km intervals based on 10,000 Monte Carlo replicates. The top of the Morgantown Tuscarora is expected to be approximately 3 km depth, which corresponds to a mean of 88 °C and 5% and 95% estimates of [72.5, 104] °C.

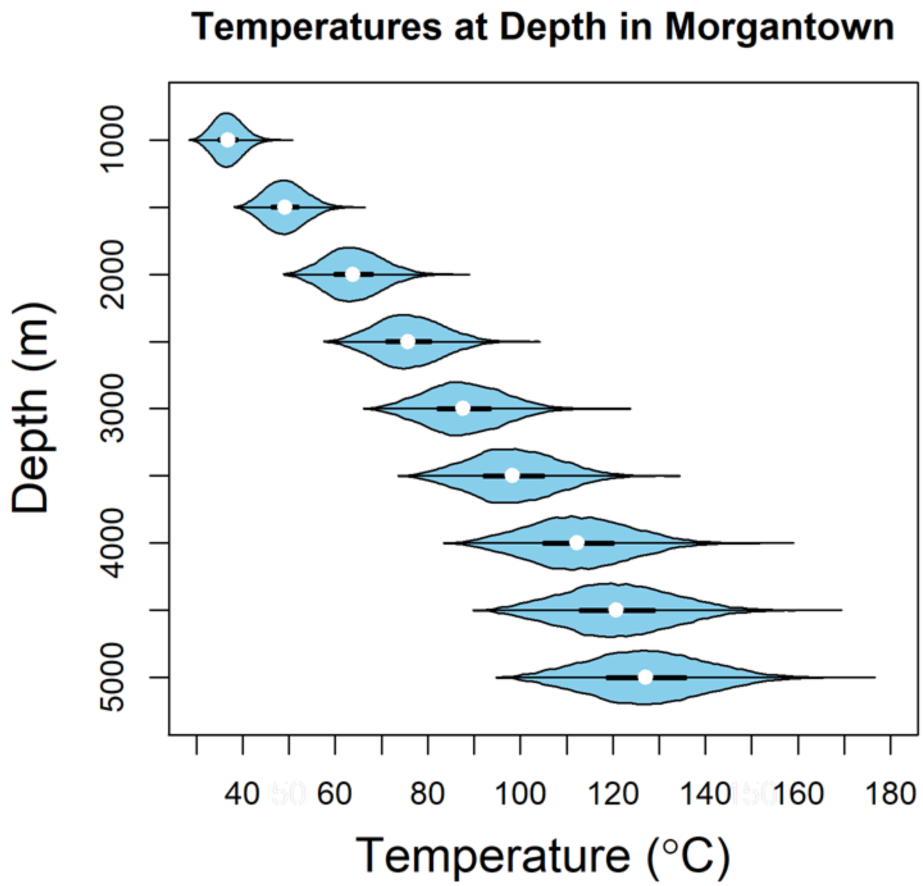

Figure 7: Estimated temperatures at depth below Morgantown, WV in 0.5 km depth increments. Violin plots (smoothed histograms) have white dots at the median temperature, and a black box in the center that spans the 25th to the 75th percentile estimates from the Monte Carlo analysis described in Section 3.5.

The temperatures as a function of depth are used to estimate the viscosity as a function of depth using the equation provided in the GEOPHIRES software (Beckers and McCabe, 2018) (Equation 5)

$$\mu = 2.414\mathrm{E}^{-5} * 10^{\left[\frac{247.8}{T+273.15-140}\right]} \tag{5}$$

where T is the water temperature (°C) and μ is the dynamic viscosity (Pa - s). The corresponding distribution of viscosity at depth is provided in Figure 8. The change in viscosity with increasing temperature is progressively smaller, so the uncertainty in viscosity decreases with increasing depth, despite increasing uncertainty in the temperature with increasing depth. The mean of the dynamic viscosity at the Tuscarora depth of 3 km depth is 3.22×10^{-4} Pa-s and the standard deviation is 3.35×10^{-5} Pa-s. This standard deviation maps to an uncertainty level of 4 for a normal distribution, which states that 2 standard deviations from the mean corresponds to values that are ±20% of the mean.

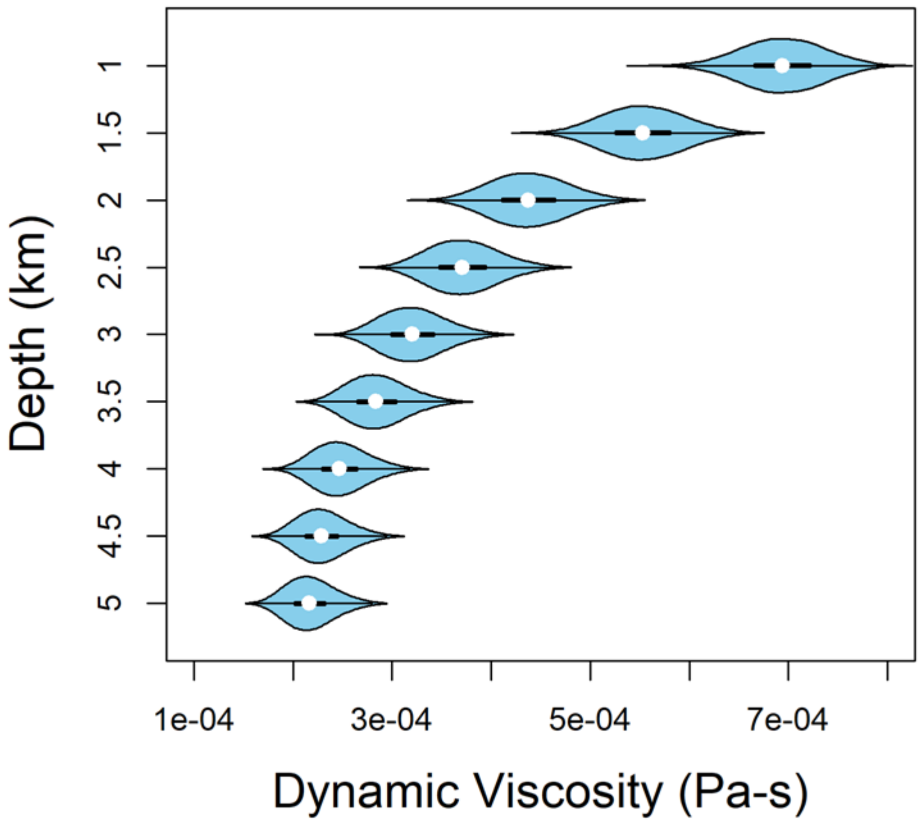

Figure 8: Dynamic viscosity of pure water as a function of depth below Morgantown, estimated using Figure 7 temperature estimates in Equation 5.

4. Monte Carlo Analysis Results for RPI_w and RFC

A Monte Carlo analysis using 100,000 replicates was used to estimate the RFC and RPI_w for the Tuscarora Sandstone below Morgantown. Table 2 provides a summary of the values and probability distributions selected for each variable. Water permeability for Matrix Rock (Figure 5) is used to compute the RPI_w metric, and water permeability for fracture-dominated flow (Figure 6) is used to compute the RFC metric.

4.1 Matrix-Dominated Reservoir Productivity

The distribution of Monte Carlo replicates for the RPI_w is provided in Figure 9, colored by the Camp et al. (2018) favorability scale. About 11% of the RPI_w estimates are in the "Favorable" range, and the rest are in the "Okay" range. Using instead the RFC with Matrix Rock permeability rates the Tuscarora as "Favorable" (Figure 10). Only 1% of the replicates are "Okay", and about 0.6% of the replicates are "Very Favorable." Thus, using the favorability thresholds and well separation distance of Camp et al. (2018), for the same dataset there is a difference in favorability using these reservoir productivity metrics. Overall, considering a matrix-dominated flow scenario, the Tuscarora below Morgantown is estimated to have favorable or okay productivity, on average, and there is a small chance that productivity will be very favorable.

Table 2: Values and probability distributions selected for the Monte Carlo analyses of the RFC and RPI_w metrics. Uncertainty levels are from Camp et al. (2018).

Variable	Distribution	Mean	Uncertainty Level
Water Permeability	Lognormal	Matrix Rock: 2.79 mD Fracture-Dominated Arithmetic Mean: 157 mD Geometric Mean: 5.2 mD	3: real-space CV = 50% 2: real-space CV = 25% 1: real-space CV = 12.5%
Reservoir Thickness	Triangular	Scenarios: 122 m or 83 m	1: Lower and upper bounds are ± 20% of the mean
Water Dynamic Viscosity	Normal	3.22×10^{-4} Pa-s	4: mean ± 2 standard deviation values are ± 20% of the mean
Water Density	Constant	988 kg/m^3	NA
Well Inner Radius	Constant	0.1 m	NA
Well Separation Distance	Constant	Scenarios: 400, 600, 800, and 1000 m	NA
Reservoir Depth	Constant	3000 m	NA
Reservoir Porosity	Constant	3%	NA

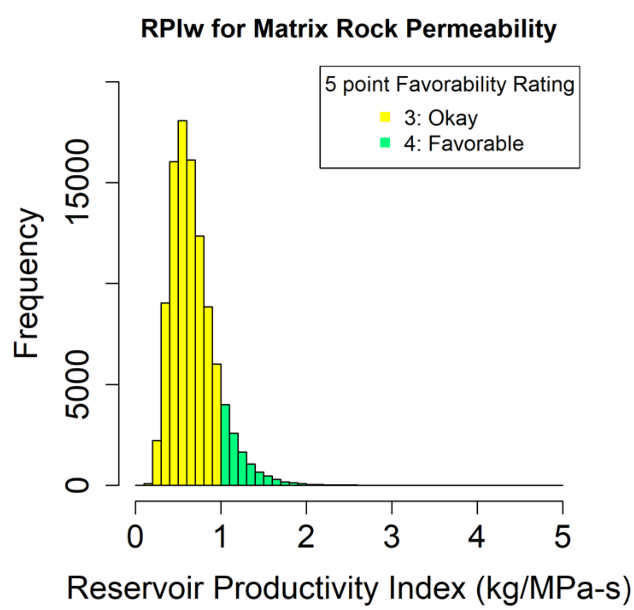

Figure 9: Reservoir Productivity Index for water (RPI_w) for Matrix Rock permeability based on 100,000 Monte Carlo replicates. The distribution is colored by the Camp et al. (2018) favorability scale for flow through reservoirs: 3: 0.1 kg/MPA-s – 1 kg/MPA-s, 4: 1 kg/MPA-s – 10 kg/MPA-s.

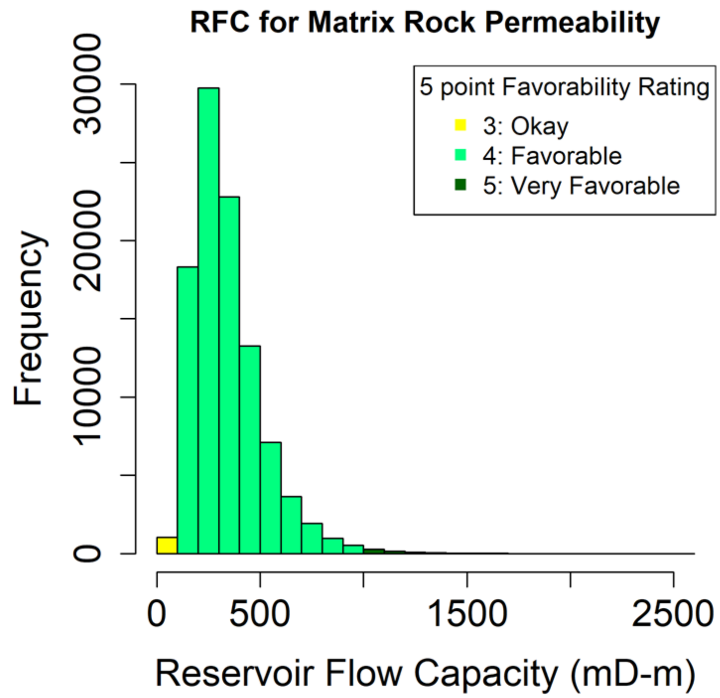

Figure 10: Reservoir flow capacity (RFC) for Matrix Rock permeability based on 100,000 Monte Carlo replicates. The distribution is colored by the Camp et al. (2018) favorability scale for flow through reservoirs: 3: 10 mD-m – 100 mD-m, 4: 100 mD-m – 1000 mD-m, 5: >1000 mD-m.

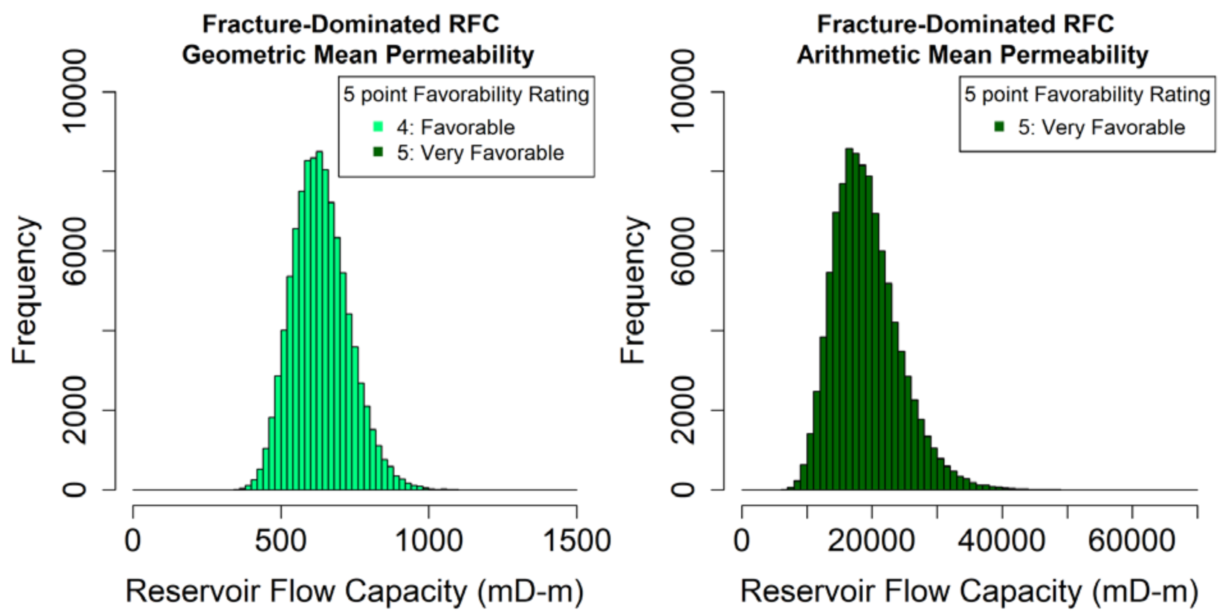

Figure 11: Reservoir flow capacity (RFC) for fracture-dominated Tuscarora based on 100,000 Monte Carlo replicates (left: geometric mean effective water permeability, right: arithmetic mean). The distributions are colored by the Camp et al. (2018) favorability scale. Values >1000 mD-m are in the "Very Favorable" category.

4.2 Fracture-Dominated Reservoir Productivity

Figure 11 provides the distributions of Monte Carlo replicates for the fracture-dominated RFC using the bootstrapped arithmetic and geometric mean effective water permeability. For the arithmetic mean, all replicates are in the “Very Favorable” range. For the geometric mean, nearly all replicates are in the “Favorable” range. Therefore, if the Tuscarora reservoir below Morgantown has fracture-dominated permeability similar to the Preston-119 permeability distribution (Figure 5), the reservoir productivity is expected to at least be favorable.

4.3 Sensitivity of the RPI_w Metric to Well Separation Distance and Reservoir Thickness

The effect of well separation and reservoir thickness on the RPI_w metric for Matrix Rock is provided in Figure 12, which shows empirical cumulative distribution functions (CDFs) of the RPI_w Monte Carlo replicates. Although the trend is expected, that a thinner reservoir provides a smaller RPI_w, and shorter well spacing provides a larger RPI_w (Equation 2), the impact of well spacing on favorability is small for the values used in this analysis. For a 122 m thick reservoir, the percentage of replicates above a “Favorable” 1 kg/MPa-s is about 11% for 1000 m spacing, and about 17% for 400 m well spacing. The impact of mean reservoir thickness is of greater importance than the well spacing for the values selected. For a 1000 m well spacing, the percentage of replicates above 1 kg/MPa-s is about 11% for a 122 m mean reservoir thickness, and about 1% for an 83 m mean reservoir thickness.

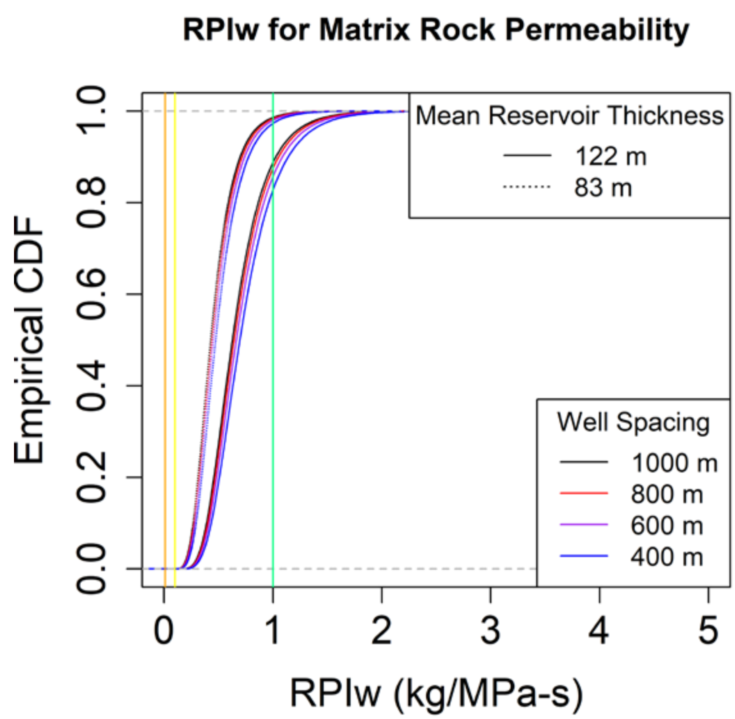

Figure 12: Empirical CDFs of computed RPI_w values for Matrix Rock using the specified mean reservoir thicknesses and well spacings in Monte Carlo analyses. Relevant favorability thresholds are shown as vertical lines. From left to right, they represent: start of “Unfavorable” region (orange), start of “Okay” region (yellow), and start of “Favorable” region (light green).

4.4 Sensitivity of the RFC Metric to Reservoir Thickness and Permeability Uncertainty Level

Figure 13 provides CDFs of the RFC metric for fracture-dominated Tuscarora as a function of the permeability uncertainty level and mean reservoir thickness specified in the Monte Carlo analyses. Considering only the impact on productivity favorability, for the arithmetic mean it does not matter which reservoir thickness or permeability uncertainty is selected because all of the Monte Carlo replicates are in the "very favorable" region. For the geometric mean, nearly all results are in the favorable region, with a small chance of being in the very favorable region for a 122 m thick reservoir.

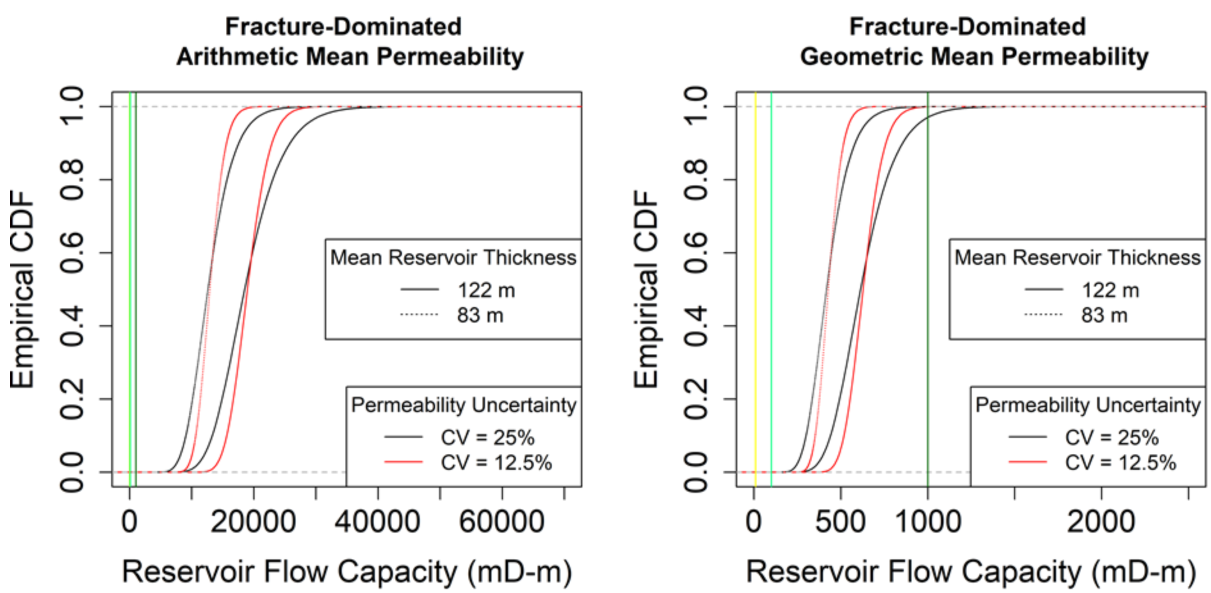

Figure 13: Empirical CDFs of computed RFC values using the specified mean reservoir thicknesses and permeability uncertainties in Monte Carlo analyses. Favorability thresholds are shown as vertical lines. From left to right, they represent: start of "Okay" region (yellow), start of "Favorable" region (light green), and start of "Very Favorable" region (dark green).

5. Appalachian Basin Reservoir Favorability and Uncertainty Maps

For matrix-dominated Tuscarora permeability, the RPI_w reservoir favorability is "Okay" on average, and might be "Favorable" using the Camp et al. (2018) favorability scale (Figure 9). Figure 14 provides the mean RPI_w favorability map and uncertainty map for the Appalachian Basin. The uncertainty is the coefficient of variation (CV) for the real-space data. A matrix-dominated Morgantown Tuscarora is estimated to be among the more favorably productive reservoirs in the basin, even for this relatively low permeability scenario.

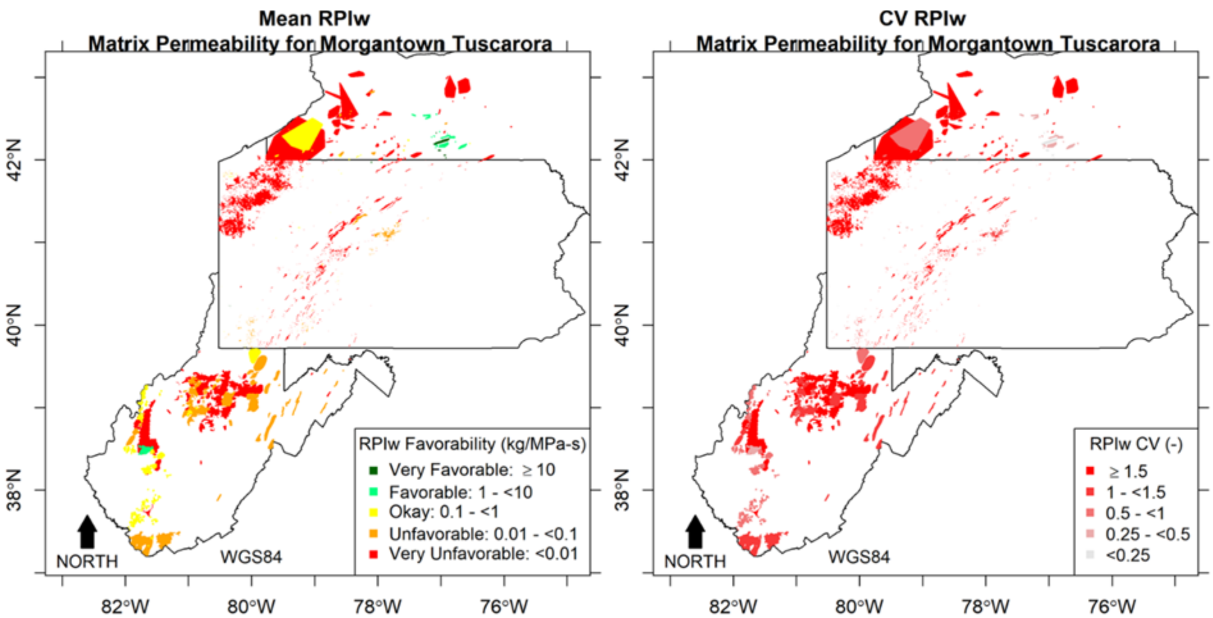

Figure 14: Map of the mean (left) and CV (right) for the RPI_w for reservoirs in Camp et al. (2018), and the Morgantown Tuscarora. Reservoirs are colored by their favorability. More favorable reservoirs are plotted on top of less favorable reservoirs where they overlap in space. Locations without reservoirs in the Camp et al. (2018) database are shown as white.

For fracture-dominated Tuscarora permeability, the RFC reservoir productivity is “Very Favorable” with no uncertainty in the favorability value for the arithmetic mean permeability, and is “Favorable” for the geometric mean permeability (Figure 11). If a fracture-dominated Morgantown Tuscarora reservoir has permeability similar to the Preston 119 Tuscarora, it is estimated to be one of few favorable to very favorable reservoirs with low uncertainty in the Appalachian Basin (Figure 15).

6. Discussion and Conclusions

This paper presented a stochastic evaluation of geothermal reservoir productivity for the Tuscarora Sandstone below Morgantown, WV. Statistical analyses of available local and regional datasets were used to characterize probability distributions of reservoir and fluid properties. A Monte Carlo uncertainty analysis of these property values allowed for probabilistic interpretations of the Tuscarora reservoir meeting flow productivity favorability thresholds. For the Morgantown Tuscarora with these datasets, the minimum flow favorability resulting from matrix-dominated permeability is expected to be “okay”, with a small chance to be “favorable” according to the Camp et al. (2018) flow productivity favorability scale. The maximum flow favorability resulting from fracture-dominated permeability is expected to be “favorable” to “very favorable,” depending on the fracture flow geometry. In terms of the flow productivity favorability used in this study, a fracture-dominated Morgantown Tuscarora would be among the most favorable and least uncertain reservoirs to develop of those identified in the Appalachian Basin by Camp et al. (2018). The analysis in this paper considers only favorability in flow, not in heat extraction. Future work could address the heat extraction favorability of the Tuscarora reservoir using the results of the statistical analyses presented in this paper.

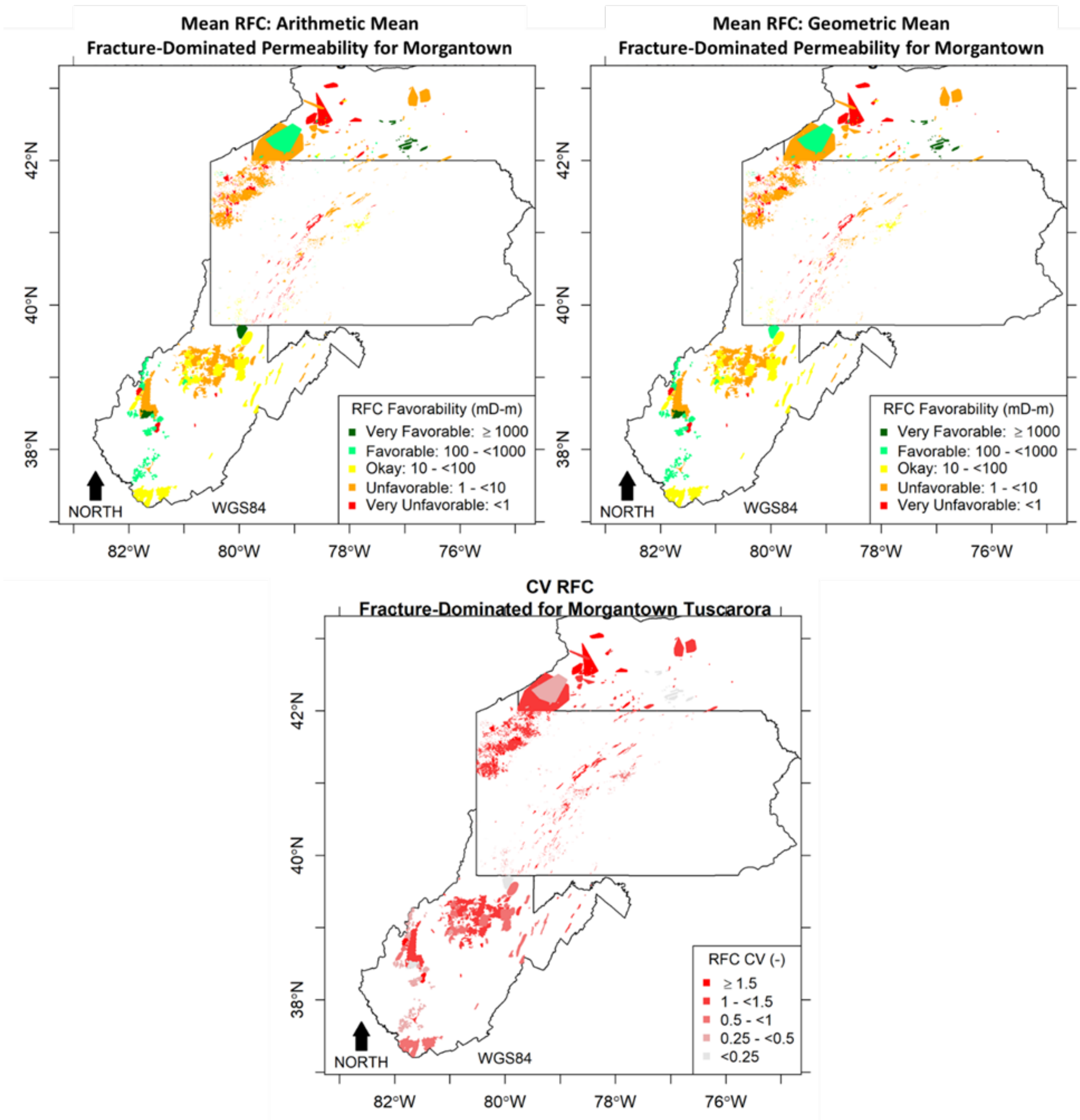

Figure 15: Map of the mean RFC for reservoirs in Camp et al. (2018), and the Morgantown Tuscarora with arithmetic mean (top left) and geometric mean (top right) fracture-dominated permeability. Only the Morgantown Tuscarora differs in the top two maps. Reservoirs are colored by their favorability, and more favorable reservoirs are plotted on top of less favorable reservoirs where they overlap in space. The CV is provided in the bottom map. The CV values for the Morgantown Tuscarora are within the same color range using either the arithmetic mean or geometric mean, so only one map is provided.

Using a sensitivity analysis for well spacing and for variables whose probability distributions are not well-characterized by the available data was useful to examine the impact of such epistemic uncertainties on Tuscarora reservoir favorability. For this dataset, considering only the impact on flow favorability, well spacing uncertainty had a smaller impact on matrix productivity than the uncertainty in the mean reservoir thickness. Uncertainty in the probability distribution parameters for permeability had a small impact on fracture-dominated favorability. Based on these results, future research and data collection efforts for Morgantown could target the largest uncertainty of whether or not Tuscarora flow productivity is fracture or matrix dominated.

This study relied on simple metrics to estimate reservoir productivity. Using the statistical methods presented in this paper and in Camp et al. (2018), these metrics can be computed before site-specific data are available to characterize the reservoir flow geometry to allow for probabilistic interpretations of a reservoir meeting certain favorability targets. The uncertainty and sensitivity analyses presented in this paper are cheap to complete relative to the expense of drilling a geothermal well in a site of interest. These stochastic analyses can inform economic decisions for proceeding into further phases of geothermal projects.

Acknowledgements

The work presented in this paper was supported by the U.S. Department of Energy's Office of Energy Efficiency and Renewable Energy under the Geothermal Technologies Office for a feasibility study of geothermal deep direct-use at the West Virginia University campus (Award Number DE-EE0008105). The author thanks the members of the West Virginia University project team, particularly Nagasree Garapati, R. Scott McCleery, and West Virginia Geological and Economic Survey team members Ron McDowell and Jessica Moore, for sharing data and for discussions about the Tuscarora Sandstone. The author thanks Teresa Jordan for reviewing an earlier version of this paper.

Software Credits and Code and Data Availability

The code and data used to complete analyses in this paper are available from the author upon email request: jds485@cornell.edu.

Data processing and statistical analyses were completed using the R language for statistical computing (R Core Team, 2018) (version 3.5.0), along with the packages GISTools (Brunsdon and Chen, 2014), Hmisc (Harrell et al., 2018), readxl (Wickham and Bryan, 2018), rgdal (Bivand, Keitt, and Rowlingson, 2018), sp (Pebesma and Bivand, 2005), stringi (Gagolewski et al., 2018), stringr (Wickham, 2018), vioplot (Adler, 2005), and writexl (Ooms, 2018). Quantum GIS (QGIS Development Team, 2018) (version 2.18.15) was used for basic spatial data processing to create the Tuscarora reservoir polygon for Morgantown.

REFERENCES

Adler, D.. (2005). vioplot: Violin plot. R package version 0.2. http://wsopuppenkiste.wiso.uni-goettingen.de/~dadler

Avary, K.L.. (1996). The Lower Silurian Tuscarora Sandstone fractured anticlinal play. In J.B. Roen, and B.J. Walker. Eds. The atlas of major Appalachian gas plays. West Virginia Geological and Economic Survey, Publication V-25, Pp. 151 - 155.

Beckers, K. and K. McCabe. (2018). GEOPHIRES. Online GitHub Repository. https://github.com/kfbeckers/GEOPHIRES.

Bivand, R., T. Keitt, and B. Rowlingson. (2018). rgdal: Bindings for the 'Geospatial' Data Abstraction Library. R package version 1.3-3. https://CRAN.R-project.org/package=rgdal

Brunsdon, C., and H. Chen (2014). GISTools: Some further GIS capabilities for R. R package version 0.7-4. https://CRAN.R-project.org/package=GISTools

Camp, E., T.E. Jordan, M.J. Hornbach, and C.A. Whealton. (2018). A probabilistic application of oil and gas data for exploration stage geothermal reservoir assessment in the Appalachian Basin. Geothermics, 71. Pp. 187 – 199.

Craft, B.C., and M.F. Hawkins. (1959). Applied Petroleum Reservoir Engineering. Englewood Cliffs, NJ, Prentice Hall.

Dietz, D.N.. (1965). Determination of average pressure from build-up surveys. Journal of Petroleum Technologies. p. 955-959.

Ehrenberg, S.N., and P.H. Nadeau. (2005). Sandstone vs. carbonate petroleum reservoirs: A global perspective on porosity-depth and porosity-permeability relationships. AAPG Bulletin, 89(4). Pp. 435 - 445.

Gagolewski, M., et al. (2018). R package stringi: Character string processing facilities. http://www.gagolewski.com/software/stringi/. DOI:10.5281/zenodo.32557

Garapati, N., O.B. Alonge, L. Hall, V.J. Irr, Y. Zhang, J.D. Smith, P. Jeanne, and C. Doughty. (2019). Feasibility of development of geothermal deep direct-use district heating and cooling system at West Virginia University campus-Morgantown, WV. Proceedings of the 44th Workshop on Geothermal Reservoir Engineering, Stanford, CA, February 11-13.

Gringarten, A.C.. ed. (1978). Geothermics and Geothermal Energy. Springer. p. 297-308.

Harrell, F.E., Jr., C. Dupont, et al.. (2018). Hmisc: Harrell miscellaneous. R package version 4.1-1. https://CRAN.R-project.org/package=Hmisc

Hennen, R.V., D.B. Reger, and W.A. Price. (1914). Preston County: Geologic report and maps. West Virginia Geological and Economic Survey County Geologic Report CGR-24. 566 p.

Jensen, J.L.. (1991). Use of the geometric average for effective permeability estimation. Mathematical Geology, 23(6). Pp. 833 - 840.

Jones, S.C.. (1987). Using the inertial coefficient, β, to characterize heterogeneity in reservoir rock. SPE Annual Technical Conference and Exhibition, Dallas, Texas, Sept. 27–30. SPE-16949-MS. http://dx.doi.org/10.2118/16949-MS.

Jones, F.O. and W.W. Owens. (1980). A laboratory study of low-permeability gas sands. J. Pet. Technol. 32 (9). pp. 1631–1640. SPE-7551-PA. http://dx.doi.org/10.2118/7551-PA.

Jordan, T.E., F.G. Horowitz, J.R. Stedinger, J.W. Tester, E.R. Camp, C.A. Whealton, J.D. Smith, B.J. Anderson, K. Welcker, X. He, M.C. Richards, C. Chickering-Pace, M. Hornbach, Z.S. Frone, C. Ferguson, R. Bolat, and M.B. Magnani. (2016). Low temperature geothermal play fairway analysis for the Appalachian Basin: Phase 1 Revised Report. U.S. Dept. of Energy Award No. DE-EE0006726. DOI: 10.2172/1341349

Lowry, T.S., J.T. Finger, C.R. Carrigan, A. Foris, M.B. Kennedy, T.F. Corbett, C.A. Doughty, S. Pye, and E.L. Sonnenthal. (2017). Reservoir maintenance and development task report for the DOE geothermal technologies office GeoVision study. Sandia National Labs Report SAND2017-9977. 81 p.

Lu, S.-M.. (2018). A global review of enhanced geothermal system (EGS). Renewable and Sustainable Energy Reviews, 81. Pp. 2902 - 2921.

McCleery, R.S., J.P. Moore, R.R. McDowell, N. Garapati, T.R. Carr, and B.J. Anderson. (2018). Development of 3-D geological model of Tuscarora Sandstone for feasibility of deep direct-use geothermal at West Virginia University's main campus. GRC Transactions, 42. Pp. 192 - 208.

McDowell, R., compiler. (2018). Summary of petrographic observations, Silurian Tuscarora Sandstone interval - Clay 513 drill core [dataset]. West Virginia Geological and Economic Survey.

McDowell, R., J. Lewis, and G. Daft, compilers. (2018). Permeability data acquired by direct air injection from the Silurian Tuscarora Sandstone interval – Preston 119 drill core [dataset]. West Virginia Geological and Economic Survey.

Ooms, J.. (2018). writexl: Export data frames to Excel 'xlsx' format. R package version 1.0. https://CRAN.R-project.org/package=writexl

Pebesma, E.J., and R.S. Bivand. (2005). Classes and methods for spatial data in R. R News 5 (2), https://cran.r-project.org/doc/Rnews/

QGIS Development Team (2018). QGIS Geographic Information System. Open Source Geospatial Foundation Project. http://qgis.osgeo.org

R Core Team. (2018). R: A language and environment for statistical computing. R Foundation for Statistical Computing. Vienna, Austria. https://www.R-project.org/

Smith, J.D.. (2019). Exploratory spatial data analysis and uncertainty propagation for geothermal resource assessment and reservoir models. Ph.D. Thesis. Cornell University. 276 p.

Smith, J.D. and F.G. Horowitz. (2017). Thermal Model Methods and Well Database Organization in GPFA-AB. In Final Report: Low Temperature Geothermal Play Fairway Analysis for the Appalachian Basin. pp. 202–234.

Solow, A.R.. (1985). Bootstrapping correlated data. Mathematical Geology, 17(7). Pp. 769 - 775.

Terry, R.D., and G.V. Chilingar. (1955). Summary of "Concerning some additional aids in studying sedimentary formations" by M.S. Shvetsov. Journal of Sedimentary Petrology, 25(3). Pp. 229 – 234.

Warren, J.E., and H.S. Price. (1961). Flow in heterogeneous porous media. SPE 1579-G. pp. 153-169.

West Virginia GIS Technical Center. (2010). Census Incorporated Places. WV State GIS Data Clearinghouse. http://wvgis.wvu.edu/data/data.php.

Wickham, H.. (2018). stringr: Simple, consistent wrappers for common string operations. R package version 1.3.1. https://CRAN.R-project.org/package=stringr

Wickham, H., and J. Bryan (2018). readxl: Read Excel files. R package version 1.1.0. https://CRAN.R-project.org/package=readxl

Witter, J.B., W.J. Trainor-Guitton, and D.L. Siler. Uncertainty and risk evaluation during the exploration stage of geothermal development: A review. Geothermics, 78. Pp. 233 - 242.